SCIENTIFIC REPORTS

OPEN

SUBJECT AREAS:
FLUID DYNAMICS
MECHANICAL ENGINEERING

Received
11 June 2014

Accepted
30 October 2014

Published
20 November 2014

Correspondence and requests for materials should be addressed to A.K. (aloke.kumar@ualberta.ca)

Formation and post-formation dynamics of bacterial biofilm streamers as highly viscous liquid jets

Siddhartha Das[1] & Aloke Kumar[2]

[1]Department of Mechanical Engineering, University of Maryland, College Park, MD 20742, USA, [2]Department of Mechanical Engineering, University of Alberta, Edmonton, Alberta, Canada T6G 2G8.

It has been recently reported that in presence of low Reynolds number ($Re \ll 1$) transport, preformed bacterial biofilms, several hours after their formation, may degenerate in form of filamentous structures, known as streamers. In this work, we explain that such streamers form as the highly viscous liquid states of the intrinsically viscoelastic biofilms. Such "viscous liquid" state can be hypothesized by noting that the time of appearance of the streamers is substantially larger than the viscoelastic relaxation time scale of the biofilms, and this appearance is explained by the inability of a viscous liquid to withstand external shear. Further, by identifying the post formation dynamics of the streamers as that of a viscous liquid jet in a surrounding flow field, we can interpret several unexplained issues associated with the post-formation dynamics of streamers, such as the clogging of the flow passage or the exponential time growth of streamer dimensions. Overall our manuscript provides a biophysical basis for understanding the evolution of biofilm streamers in creeping flows.

The normal form of bacterial growth in most environments is now recognized to occur as a biofilm, which is a social form of growth associated with solid phase surfaces[1–4]. Biofilms include differentiated populations of cells embedded in a matrix of self-produced extracellular polymeric substances (EPS)[5,6], displaying physiological properties that vary significantly from that of a dispersed cell population. Biofilms have attracted significant interdisciplinary attention as they can lead to persistent infections[7,8], fouling of surfaces[9,10], and at the same time help in waste-water treatment[11].

Biofilms are excellent examples of viscoelastic materials[12,13], exhibiting a complex range of behaviors to external force including deformation, fracture and strain-hardening[6]. Recently, multiple researchers have demonstrated that even in low Reynolds number ($Re \ll 1$) flows, appearance of surface-hugging biofilms was followed, after a time lag of several hours, by the appearance of filamentous structures (extruding from the pre-formed biofilms) known as streamers[14–19]. These streamers that we study here are in creeping ($Re \ll 1$) background flow (e.g., $Re \sim 0.1$ in Rusconi et al.[15] and Drescher et al.[20] and $Re \sim 0.01$ in Valiei et al.[17]) and hence are distinctly different from the streamers formed in turbulent background flow in a multitude of scenarios[21–27]. Streamer formation in low Re has wide repercussions as they can act as precursors to the formation of mature biofilms in complex microstructures[17,20], lead to more rapid and catastrophic clogging of devices[20], cause substantial flow-structure interactions[28], etc. Despite the recent interests in biofilm streamer dynamics, there remain several open questions, e.g., What is the effect of biofilm rheology in streamer formation? What is the reason for the substantial time lag between the formation of biofilms and the appearance of streamers? How can one explain different effects associated with the post-formation dynamics of streamers, such as the rapid clogging of the flow device[20], or the very fast growth of the streamer dimensions with time[15]?

In this work, we provide answers to all of the above questions. We start by explaining that the streamers form as the "*viscous liquid*" state of the intrinsically viscoelastic biofilms, with shear modulus G, viscosity μ_b and the viscoelastic relaxation time $\tau_{ve} = \mu_b/G$ (see Fig. 1 and Supplementary Information section 1). Such a hypothesis allows us to explain the large time lag (henceforth denoted as t_s) between the formation of the biofilms and the appearance of the streamers, and at the same time quantify the role of biofilm rheology in streamer formation. This hypothesis is also corroborated by the experimental signature of streamer formation, which suggests the involvement of extrusion process (Fig. 2). Being in the "*viscous liquid*" state, the biofilms fail to resist the flow-driven shear forces (often too weak to cause any substantial elastic extrusion) resulting in degeneration as streamers. Secondly, we explain the post-formation dynamics of the streamers as that of a highly viscous liquid

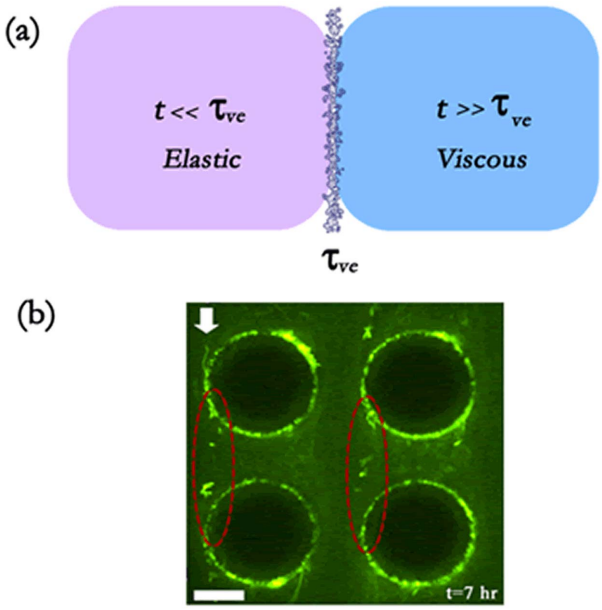

Figure 1 | (a) Pictorial representation of the proposed hypothesis that streamers form as viscous liquid jets. (b) We show green fluorescent bacteria forming a streamer (demarcated by dashed ellipses). Flow is from top to bottom as shown by arrow. Scale bar is 20 μm (experimental set up identical to that of Valiei et al.[17]). Streamers form several hours after the start of formation of the biofilms and directional growth is not observed. Also the biofilms employed here are formed from *Pseudomonas fluorescence* bacterium – these biofilms are considered to have viscoelastic relaxation time of a few minutes.

jet in a background flow. In case the background flow can be approximated to be co-axial to the streamer jet transport, we demonstrate that the typical conditions pertaining to streamer formation[15–18,20] will lead to "absolute instability"[29,30] of the streamer liquid jet, enforcing the jet to break down into smaller drops. We derive scaling relationships to quantify the breakup length characterizing such breakup, and demonstrate that these lengths are often too large to cause any drop formation in microfluidic systems studying streamer formation[17]. On the contrary, dictated by the geometry, if the streamer jet is in "*crossflow*" to the background flow[20], the streamers break down into drops almost instantly after their formation. This can explain the unbroken filamentous morphology of streamers in the experiment of Valiei et al.[17], and at the same time account for the "porous-matrix-like" structure inside the flow domain witnessed in the experiment of Drescher et al.[20]. Finally, we establish that only by considering the streamers to evolve as viscous drops, we can quantify effects such as exponential increase in streamer dimensions[15,20] and catastrophic clogging of flow devices.

Results

Post-formation streamer dynamics - streamers as highly viscous liquid jets. Our primary hypothesis is that streamers are formed when the biofilm attains a "viscous" state. Basis of this hypothesis is that the biofilms are viscoelastic liquids (with relaxation time τ_{ve}) and the time scale of streamer formation is substantially larger than τ_{ve} (see Table I, *Discussions* section, Supplementary Information sections I, II, Tables I and II in Supplementary Information). Streamers being formed from the "viscous liquid" biofilms, their post-formation dynamics can be interpreted as that of highly viscous liquid jets moving through a background flow. This dynamics depends on the direction of the background flow with respect to the direction of the streamer jet. In case the background flow is in the same direction as that of the streamers, we can invoke

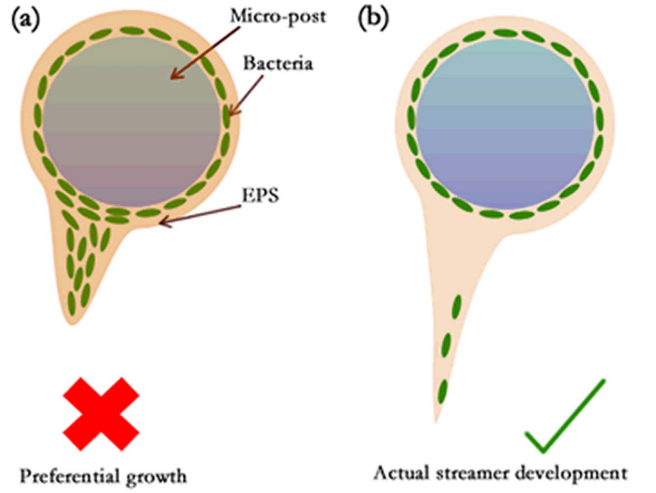

Figure 2 | **Schematic showing the expected difference in biofilm growth between the cases where the growth occurs due to (a) directional growth and (b) extrusion/flow.**

the study of Guillot et al.[29,30] to describe the streamer dynamics: we perform stability analysis of the streamers, represented by a thin cylindrical viscous jet of viscosity μ_b and radius R_s, moving coaxially with a flow (of viscosity μ_f) inside a capillary of radius ξ (see section III and Fig.1 in Supplementary Information). The instability equation, characterized by the parameters $Ka = (-\partial p/\partial z)\xi^2/\gamma = \mu_f u_c/\gamma$ ($\partial p/\partial z$ is the pressure gradient, u_c is the characteristic speed of the surrounding liquid, γ is the surface tension between the streamer liquid and the bulk liquid and Ka is an effective capillary number at the scale of the capillary) and ratios R_s/ξ and μ_b/μ_f, can be expressed as (see Refs. 29, 30 and section III and Fig. 1 in Supplementary Information):

$$Ka = \frac{C_1 F\left(\frac{R_s}{\xi}, \frac{\mu_b}{\mu_f}\right)}{\left(\frac{R_s}{\xi}\right)^3 E\left(\frac{R_s}{\xi}, \frac{\mu_b}{\mu_f}\right)}, \tag{1}$$

where $C_1 = \frac{5+\sqrt{7}}{18}\sqrt{\frac{24}{\sqrt{7}-1}}$ and E and F are functions, expressed as:

$$E\left(\frac{R_s}{\xi}, \frac{\mu_b}{\mu_f}\right) = -4\left(\frac{R_s}{\xi}\right) + \left(8 - \frac{\mu_f}{\mu_b}\right)\left(\frac{R_s}{\xi}\right)^3 + 4\left(\frac{\mu_f}{\mu_b} - 1\right)\left(\frac{R_s}{\xi}\right)^5, \tag{2}$$

$$F\left(\frac{R_s}{\xi}, \frac{\mu_b}{\mu_f}\right) = \left[4 - \frac{\mu_f}{\mu_b} + 4\ln\left(\frac{R_s}{\xi}\right)\right]\left(\frac{R_s}{\xi}\right)^4 + \left(-8 + \frac{4\mu_f}{\mu_b}\right)\left(\frac{R_s}{\xi}\right)^6 + \left[4 - \frac{3\mu_f}{\mu_b} - 4\left(1 - \frac{\mu_f}{\mu_b}\right)\ln\left(\frac{R_s}{\xi}\right)\right]\left(\frac{R_s}{\xi}\right)^8. \tag{3}$$

Table I | Variation of the time scales τ_{ve} and t_s from the corresponding biofilms (* We invoke the property of commonality of biofilm relaxation time[13])

Bacteria forming Biofilms	τ_{ve}(min)	t_s(hours)
Pseudomonas aeruginosa	18[13]	5–10[15,16] 20–40[20]
Pseudomonas fluorescens	18*[13]	9[17]
Staphylococcus epidermis	19.2[33] 21.9–25.5[41]	6[18]

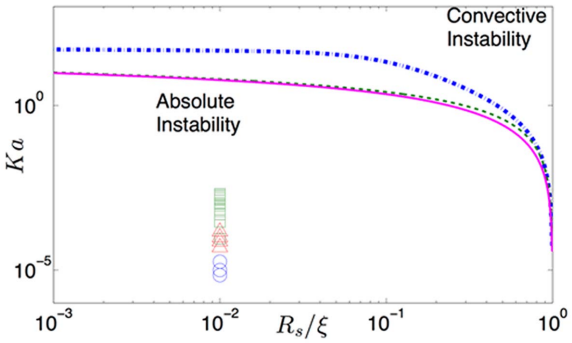

Figure 3 | Phase diagram for the instability (for a circular jet in a circular capillary) in the $Ka = (-\partial p/\partial z)\xi^2/\gamma = \mu_f u_c/\gamma$ and R_s/ξ planes for different μ_b/μ_f values (blue dashdot line for $\mu_b/\mu_f = 0.01$, green dashed line for $\mu_b/\mu_f = 1$ and magenta solid line for $\mu_b/\mu_f \geq 100$). We have convective instability above the curves and absolute instability below the curves. Absolute instability leads to spontaneous breakdown of the jet into drops. We plot the experimental results [i.e., the corresponding Ka (see Table II in Supplementary Information) and R_s/ξ or $R_s/(h/2)$ values; here h is the characteristic dimension of a possible rectangular geometry, see Supplementary Information] for different experiments (circle for Valiei et al.[17], triangles for Rusconi et al.[15] and squares for Drescher et al.[20]). Also for all the experiments $\mu_b/\mu_f = 10^7$ (since we take $\mu_f = 10^{-3}$ Pa-s and $\mu_b = 10^4$ Pa-s[13]) and we take R_s/ξ [or$R_s/(h/2)$] = 0.01. Therefore the experimental Ka and R_s/ξ values signify an absolute instability regime, which will suggest a spontaneous breakdown of the jet into droplets for all the streamer-forming experiments[15,17,20].

The resulting instability phase diagram is shown in Fig. 3. Above the lines the viscous streamer jet will be convectively unstable, whereas below the lines the jet is absolutely unstable[29,30]. The "absolute instability" regime is characterized by spontaneous breakdown of the jet into drops with the perturbations propagating both upstream and downstream. This is in contrast to the classical convective instability, where the perturbations propagate only downstream. In Fig. 3, we plot the experimental conditions (characterized by Ka and R_s/ξ values; see Table II for determination of these parameters) corresponding to the streamer formation, as reported in the literature[15,17,20]. For these experiments, we typically encounter $\mu_b/\mu_f \sim 10^7$, and accordingly these data points are located below the instability phase line, indicating that the streamer formation conditions are such that the streamer liquid jet will spontaneously break down into smaller drops, with the breakdown being characterized by the break up length l_{bs}.

Following Javadi et al.[31], we can develop a scaling argument to quantify this break up length l_{bs} for streamers in coaxial flow (see section IV in the Supplementary Information for detailed derivation) as:

$$l_{bs} \sim R_s(\mu_b u_c/\gamma). \tag{4}$$

Consequently, for the experiment of Valiei et al.[17], we get $l_{bs} \sim 100\ \mu$m (using $R_s \sim 1\ \mu$m, $\mu_b \sim 10^4$ Pa-s, $\gamma \sim 0.01$ N/m, $u_c \sim 10^{-4}$ m/s) – we indeed find that the streamers continue as long unbroken jets/filaments between two microposts having separation distance much smaller than l_{bs} (see Fig. 2 in Supplementary Information). Using the same scaling, we would get $l_{bs} \sim 1$–10 mm (employing $R_s \sim 1\ \mu$m, $\mu_b \sim 10^4$ Pa-s, $\gamma \sim 0.01$ N/m, $u_c \sim 10^{-3}$–10^{-2} m/s) for the experiment of Rusconi et al.[15] and Drescher et al.[20]. However in these experiments[15,20], as per our hypothesis, the streamer viscous jet will rapidly break down into smaller drops. This can be explained by noting that in these experiments[15,20], because of the flow passage geometry the streamer jet is not aligned to the background flow; rather, the jet can be assumed to be partly in a crossflow scenario (with respect to the background flow) (see Fig. 3 in Supplementary Information). In case the streamer jet is assumed to be completely in crossflow with the background flow, the breakup length can be expressed as (see section V and in Supplementary Information for detailed derivation):

$$\frac{l_{bs}}{\xi} - \frac{2}{3}\left(\frac{l_{bs}}{\xi}\right)^3 + \frac{1}{5}\left(\frac{l_{bs}}{\xi}\right)^5 = \frac{1}{k}\frac{R_s}{\xi}. \tag{5}$$

The principle behind the derivation is to quantify the breakup length as the length where the momenta of the background crossflow and the streamer jet balance each other. The factor k in eq.(5) depends on the choice of the velocity scale used to quantify the flow of the streamer jet – it is equal to 2 if the velocity scale of the streamer jet is equal to the average velocity (of the background flow) and is equal to 8 if the velocity scale is the maximum velocity (of the background flow). l_{bs} computed from eq.(5) can become even smaller than R_s (see section V and Fig. 4 in Supplementary Information) - therefore the drop formation (from streamers) is caused by the presence of geometry-induced crossflow elements[15,20]. Presence of such drops and its corresponding growth owing to the mass addition (see below) ensures the "porous-matrix-like" structure inside the flow domain[20].

Time variation of streamer dimensions. The key physics behind the temporal variation of the streamer dimensions, as explained by Drescher et al.[20], is the addition of mass to the streamers by the incoming cells. In their experiments, Rusconi et al.[15] reported a close to exponential (for small times) increase in the streamer dimensions with time. They also reported a smaller streamer dimension at a given time for a weaker flow rate. Drescher et al.[20] demonstrated that the time scale for this exponential streamer growth varies as 1/(flow rate). Analysis of Drescher et al.[20], considering streamers as a "solid" body, cannot recover this exponential behavior - on the contrary, their analysis will exhibit a growth dynamics expressed as (see section VI in the Supplementary Information):

$$\frac{R_s}{R_{s,0}} = \frac{1}{1 - t/\tau_{theory,1}}, \tau_{theory,1} = \frac{7\mu_f}{\beta C \Delta p A_{ac} R_{s,0}}. \tag{6}$$

Table II | Variation of the capillary number (Ka) for different experiments on streamer formation. For all the cases, we consider $\mu_f \sim 10^{-3}$ Pa−s and $\gamma = 0.01$ N/m. Also $\mu_b \sim 10^4$ Pa−s[13], so that $\mu_b/\mu_f = 10^7$. Here we tabulate all the possible Ka corresponding to the different flow rates employed in a given experiment

Experiment	Q (μL/min)	u_c (mm/s)	$Ka \times 10^4$
Rusconi et al.	0.5, 0.75, 1.0, 1.5	0.49, 0.74, 0.98, 1.47	0.49, 0.74, 0.98, 1.47
Valiei et al.	0.13, 0.2, 0.33	0.07, 0.10, 0.18	0.07, 0.10, 0.18
Drescher et al.	0.9–20	0.83–18.5	0.83–18.5

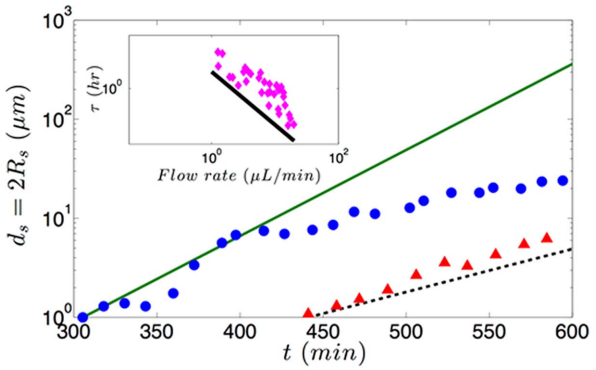

Figure 4 | Temporal variation of the streamer diameter $d_s = 2R_s$. Experimental results correspond to the streamer formation in a microchannel with 330° bend reported in the experiment of Rusconi et al.[13] for different flow rates (circles for 1 μL/min and triangles for 0.5 μL/min). The continuous lines (solid line for flow rate for 1 μL/min and dashed line for 0.5 μL/min) are the theoretical predictions using an exponential variation expressed as $R_s/R_{s,0} = d_s/d_{s,0} = \exp[(t-t_0)/\tau_{theory,2}]$ [this is a modification of eq.(2), considering $d_s(t = t_0) = d_{s,0}$; here $d_{s,0}$ and t_0 are the values obtained from the experiment]. To compute $\tau_{theory,2}$, we use eq.(7), with parameters $u_c = 10^{-3}$ m/s (for flow rate 1 μL/min) and $u_c = 0.5\times10^{-3}$ m/s (for flow rate 0.5 μL/min), $C = 5 \times 10^{-4}$ cells/μm^3[15], $A_{ac} = 2$ μm^2 and $\beta = 0.67 \times 10^{-3}$. In the inset we show the variation of time scale (τ) of streamer dynamics with the flow rate. Experimental results[20] are shown by markers, whereas our prediction ($\tau_{theory,2}$) is shown by a solid line. For this prediction, we consider the same dependence of u_c on flow rate and keep all other parameters same, except for C, which is now $C = 2 \times 10^{-4}$ cells/μm^3 [20].

We rectify Drescher et al.'s analysis; we demonstrate that such exponential increase in the streamer thickness can be accounted by considering that the streamers evolve as drops. The corresponding growth dynamics can be expressed as (see section VI in the Supplementary Information):

$$\frac{R_s}{R_{s,0}} = \exp\left(t/\tau_{theory,2}\right), \tau_{theory,2} = \frac{2}{\beta C u_c A_{ac}}. \tag{7}$$

In the above equations, C is the bacterial cell concentration, A_{ac} is the area added by an advected cell to the streamer, β is the fraction of cells that get caught in the streamer, Δp is the pressure drop across the streamer (assuming it to be a "solid" cylinder), and $R_{s,0}$ is the thickness of the streamer at the time when streamer starts to form. In Fig. 4, we show the comparison of the experimental results[15] and our theoretical prediction of the temporal variation of the streamer thickness for different flow rates. For smaller flow rates (~0.5 μL/min), we get excellent agreement with the experimental results, whereas for higher flow rates (~1 μL/min) the agreement is primarily at smaller times. At larger flow rates and at substantially large times, the flow clogging mechanism induced by the streamers will cause a weaker than exponential increase of the streamer dimensions. In the inset of the Fig. 4, we compare our theoretical prediction ($\tau_{theory,2}$) with the experimental result[20] of the streamer formation time scale τ as a function of the flow rate, and recover the 1/(*flow rate*) dependence of the time scale. Such dependence is also recovered for the time scale ($\tau_{theory,1}$) corresponding to the "solid state" streamer, although the magnitude of $\tau_{theory,1}$ is substantially larger, which will fail to recover the τ values observed in experiments (see inset of Fig. 4). In this context, it is worthwhile to mention that had we considered streamers as long cylindrical liquid entities with constant length with the addition of cells increasing the surface area, we would have also got $dR_s/dt \sim R_s$, yielding an exponential growth rate of the streamers (with a time constant different from $\tau_{theory,2}$). The main limitation for such a hypothesis (i.e., considering streamers as long, cylindrical liquid entities) is that we assume that the streamers persist as stable jets, which is a notion not supported by the experimental systems (e.g., the systems of Drescher et al. [20] and Rusconi et al. [15]), where the streamer jets are in partial cross flow and this growth dynamics becomes evident and important. Contrary to the studies of Rusconi et al.[15] and Drescher et al.[20], in experimental set up of Valiei et al.[17] the streamers being coaxial to the background flow, the flow direction is tangential to the direction of axis of the cylindrical jet (which does not break into droplets, see above), and hence the transfer of cells to the streamer can only occur diffusively (with diffusivity D), yielding (see section VI in the Supplementary Information):

$$\frac{R_s}{R_{s,0}} = 1 + \frac{t}{\tau_{theory,3}}, \tau_{theory,3} = \frac{2R_{s,0}}{\beta C A_{ac} D}. \tag{8}$$

Clogging effect of streamers. As discussed by Drescher et al.[20], one of the key signatures of the streamer dynamics is the manner in which it clogs the flow by causing a substantial reduction in the flow rate. Drescher et al.[20] argued that such a behavior could be attributed to the "solid" state of the streamers and the fact that the streamers are positioned in the bulk and not at the walls. We find, on the contrary, that on being located in the bulk, the "liquid" state of the streamers may actually lead to a greater reduction in the flow rate (this flow rate is denoted as $Q_{st,l}$) for certain ranges of streamer thickness values (see section VII and Fig. 6 in the Supplementary Information). This reduction can be explained by noting (see section VII in the Supplementary Information for detailed derivation):

$$\frac{Q_{st,l}}{Q_0} = \left(1 - \frac{R_s}{\xi}\right)^4, \tag{9}$$

where Q_0 is the volume flow rate for a steady pressure-driven fully-developed flow inside a cylindrical capillary of radius ξ. This reduction gets severely more enhanced (see Fig. 6), and is manifested over the complete spectrum of the streamer thickness values, when the "viscous liquid" streamer jet, on account of geometry-induced crossflow, breaks down into smaller dimensions, which would now occupy a much larger cross sectional area of the channel. This reduction (see Fig. 5 in the Supplementary Information) can be explained from the corresponding expression of the volume flow rate. Considering that the streamer jet has broken down into 3 equal identical segments that are symmetrically placed across the capillary height, we can express the corresponding flow rate ($Q_{st,3l}$) as (see section VII in the Supplementary Information):

$$\frac{Q_{st,3l}}{Q_0} = 1 - \left(\frac{1}{2} + \frac{R_s}{\xi}\right)^2 \left[2 - \left(\frac{1}{2} + \frac{R_s}{\xi}\right)^2\right] + \left[1 - 4\left(\frac{R_s}{\xi}\right)^2 + 4\frac{\mu_f}{\mu_b}\frac{R_s}{\xi}\right] \left(\frac{1}{4} - \frac{R_s}{\xi}\right) - \left(\frac{1}{2} - \frac{R_s}{\xi}\right)^4 + \left(\frac{R_s}{\xi}\right)^4. \tag{10}$$

Discussion

Why Streamers form as "viscous liquid" state of biofilms. Biofilms are viscoelastic liquids[12,13,25,32] – therefore, at times $t \ll t_{ve}$ they exhibit a behavior analogous to elastic solids, whereas at times $t \gg t_{ve}$ they exhibit a behavior identical to that of highly viscous liquids (see section I in the Supplementary Information for a more elaborate discussion). Rheological measurements exhibit wide ranges of values of the shear modulus G and viscosity μ_b of the biofilms[12,13,25,27,33–37], although there is a remarkable commonality in the viscoelastic relaxation time $\tau_{ve} = \mu_b/G$[13] (see section I and

Table I in the Supplementary Information). In order to understand the rheological state of the biofilms that lead to streamer formation, we must compare t_s with τ_{ve}. In Table I, we summarize the t_s values corresponding to different experiments reporting the formation of streamers, as well as the corresponding τ_{ve} values (for the biofilms forming the streamers) obtained from separate rheological measurements. From this table it is clear that we always encounter $t \gg t_{ve}$, establishing the validity of our hypothesis of considering streamers as "viscous liquid" state of the biofilms (see Fig. 1 and section I in the Supplementary Information for more details). Please note that in an earlier study, Rusconi et al.[16] used this idea of $t \gg t_{ve}$ to hypothesize streamers as viscous liquid; however, they did not provide any further analysis to establish their claims. Also we shall like to distinguish between the streamers that we describe from that of the aggregation-driven streamers witnessed by Yazdi and Ardekani[19]. Our analysis negates the idea that the streamers form from the "elastic" degeneration of the biofilms[15,20,38], since the imposed elastic strain (e) from the flow shear is invariably very weak, i.e., $e \sim 10^{-2}$–10^{-4} [15–18,20] (see Table II and section II in Supplementary Information for details). On the contrary, when the biofilms attain the "viscous liquid" state, it will fail to resist any imposed shear, thereby degenerating into streamers. Note that the quantitative relationship between the strain e (or applied stress σ) and t_s, obtained from different experiments, are not well explained. In this context, it is worthwhile to point out the impact of biological growth in the streamer formation process. We shall like to emphasize here that we are not discounting biological growth based on time-scales. In fact, since streamer formation time-scales (few to several hours) are much longer than cell division time-scale (~30 min) it is not possible to rule out the role of growth based on time-scale alone. The physical basis for neglecting growth, on the contrary, is illustrated in Fig. 2. If preferential accumulation and/or growth contributed to streamer formation, then the experimental signature of streamer formation would be similar to Fig. 2a. However, in reality[17], the experimental signature is similar to the illustration in Fig. 2b. This experimental signature suggests that in the initial phase, streamer formation is dominated by mechanical response of viscoelastic biofilms to externally imposed shear.

Streamers as jets and their breakup. We have based our analysis and results under the assumption that the biofilm streamers are formed as jets of highly viscous liquids. These jets are formed by the shearing action of the background flow on the viscoelastic biofilm. In this light, streamer formation is indeed "shear-driven". Once formed, they are either in co-flow or cross-flow (partly) with the background pressure-driven transport. For the former case, in order to ensure stable base state of the jet, the axial pressure-gradient needs to be identical in both the streamer jet and the background flow and the streamer jet will be driven by an imparted shear from the background flow [see eqs.(2,3) in the Supplementary Information]. It is also important to distinguish here between the streamer jets in co-flow and cross-flow. Although like the streamers jets in co-flow, streamer jets in cross-flow also form due to the shearing action of the background transport, it need not conform to the background pressure-driven transport as is done by the jets in co-flows. This difference, as has been established here, dictate the break-up dynamics of the jet. In context of the jet break-up, we shall like to emphasize here that the jet breakup is strictly a liquid instability phenomenon. In other words, elasticity has no role to play here as evident from the fact that the corresponding elastic or elastocapillary bending length[39] $l_{EB} \sim \sqrt{GR_s^3/\gamma} \approx 30$nm (considering $G \sim 10$ Pa for *Pseudomonas aeruginosa*, $R_s \sim 1$ μm, $\gamma = 0.01$ N/m), i.e., much smaller than the break up length for jets in both co-flow and cross-flow. Had elasticity effects been important, the break up length of the jets would have been of the same order as l_{EB}. Finally, we shall like to mention here that we start with an assumption that the streamers, once formed, start with a radius $R_{s,0}$. Our theory of jet break up and growth dynamics of streamers remain valid as long as $R_{s,0}$ is finite. Exact prediction of the value of $R_{s,0}$ would require a full-scale numerical simulation, which is beyond the scope of the present study.

To summarize, we have provided a theory to establish that the biofilm streamers, witnessed at very low *Reynolds* number (Re $\ll$ 1) microfluidic transport, form as viscous liquid jets. Our theory allows us to explain the very large time scales (~several hours) associated with the streamer formation, that occurs in presence of extremely weak flow-driven shear stresses (direct experimental validation of the presented theory remains a challenging task at present). Further, our theory reproduces the experimental results[15,20] of growth dynamics of the streamers quantitatively, hitherto missing from the existing studies. Finally, it is important to note that the streamer jets, which will invariably form as viscous jets, may attain viscoelastic rheology on account of entrapment of bacterial cells that produce EPS. The time scale of this change of rheology will be similar to that of the growth of process (~hours). Hence it will not affect the initial streamer viscous jet dynamics with much smaller characteristic time - we probe this initial dynamics to explain the unbroken streamers in Valiei et al.[17] and jet-to-drop transition in Rusconi et al.[15] and Drescher et al.[20]. But at larger times, this change of rheology can help explain issues such as the $C^{0.6}$ dependence of timescale dictating the streamer growth[20], or the physical origin of the fitting factor β. Such explanation, along with those forwarded in this study will lead to a more comprehensive understanding of the biofilms in low Reynolds number hydrodynamics.

Methods

In this study, we employ different theoretical methods, which are discussed below:

- *Stability Analysis*: We have employed the *Stability Analysis* proposed by Guillot et al.[30]. The method, described in details in section III in the Supplementary Information, performs a perturbation analysis on the co-axial flow field base state (i.e., flow field that describes the transport of the highly viscous liquid streamer jet in a co-axial background microfluidic transport), provides the stability curve as a function of system parameters describing, whether or not the streamer jet will break down into drops.
- *Fluid Flow Analysis for estimating the jet breakup length*: When the viscous streamer jets are co-axial to the background flow, we employ a fluid flow analysis method similar to that proposed by Javadi et al.[31] to compute the breakup length of the streamer. The method is based on balancing the viscous stress term (highly magnified since the streamers are extremely viscous) with the background flow induced shear stresses (see section IV in the Supplementary Information for more details). In case the streamers are in cross-flow, we employ a fluid flow analysis method similar to that proposed by Muppidi and Mahesh[40] to obtain the breakup length. The method is based on computing the distance at which the momentum of the cross-flow becomes equal to the momentum of the jet – it is at this distance the jet breaks (see section V in the Supplementary Information for more details).
- *Mass balance analysis for estimating growth rate of streamer dimensions*: The streamers, assumed to evolve as liquid jets, grow in mass due to addition of advected cells. This analysis is similar to that employed by Drescher et al.[20], with two exceptions. First, it consider the streamer as a liquid jet (and not a "solid" cylinder as considered by Drescher et al.[20]) and second the mass addition is assumed to increase the surface area of the streamers and not the cross sectional area. These exceptions ensure that we do recover the experimentally observed exponential increase in the streamer growth rate (see section VI in the Supplementary Information for more details).
- *Flow rate analysis for estimating clogging action of the streamers*: The method employed here is the calculation of the net flow rate within the micro-conduit neglecting the flow inside the streamers. Calculations are done for the following cases: a) the biofilm is adhered to the conduit wall (Drescher et al. have also done this calculation[20]), b) the biofilm has extruded into a single "solid" streamer of cylindrical configuration (Drescher et al. have also done this calculation[20]), c) the biofilm has extruded into a single "liquid" streamer of cylindrical configuration and d) the biofilm has extruded into multiple "liquid" streamers (see section VII in the Supplementary Information for more details).

1. Costerton, J. W., Lewandowski, Z., Caldwell, D. E., Korber, D. R. & Lappin-Scott, H. M. Microbial biofilms. *Annu. Rev. Microbiol.* **49**, 711–745 (1995).
2. Häussler, S. & Parsek, M. R. Biofilms 2009: new perspectives at the heart of surface-associated microbial communities. *J. Bacteriol.* **192**, 2941–2949 (2010).

3. Neethirajan, S. *et al.* in *Encyclopedia of Nanotechnology* 213–219 (Springer, 2012).
4. Wong, G. C. & O'Toole, G. A. All together now: integrating biofilm research across disciplines. *MRS Bull.* **36**, 339–345 (2011).
5. Flemming, H.-C. & Wingender, J. The biofilm matrix. *Nat. Rev. Microbiol.* **8**, 623–633 (2010).
6. Wilking, J. N., Angelini, T. E., Seminara, A., Brenner, M. P. & Weitz, D. A. Biofilms as complex fluids. *MRS Bull.* **36**, 385–391 (2011).
7. Costerton, J., Stewart, P. S. & Greenberg, E. Bacterial biofilms: a common cause of persistent infections. *Science* **284**, 1318–1322 (1999).
8. Fux, C., Costerton, J., Stewart, P. & Stoodley, P. Survival strategies of infectious biofilms. *Trends Microbiol.* **13**, 34–40 (2005).
9. Callow, J. A. & Callow, M. E. Trends in the development of environmentally friendly fouling-resistant marine coatings. *Nat. Commun.* **2**, 244 (2011).
10. Lappin-Scott, H. M. & Costerton, J. W. Bacterial biofilms and surface fouling. *Biofouling* **1**, 323–342 (1989).
11. Van Loosdrecht, M. & Heijnen, S. J. Biofilm bioreactors for waste-water treatment. *Trends Biotechnol.* **11**, 117–121 (1993).
12. Klapper, I., Rupp, C., Cargo, R., Purvedorj, B. & Stoodley, P. Viscoelastic fluid description of bacterial biofilm material properties. *Biotechnol. Bioeng.* **80**, 289–296 (2002).
13. Shaw, T., Winston, M., Rupp, C., Klapper, I. & Stoodley, P. Commonality of elastic relaxation times in biofilms. *Phys. Rev. Lett.* **93**, 098102 (2004).
14. Marty, A., Roques, C., Causserand, C. & Bacchin, P. Formation of bacterial streamers during filtration in microfluidic systems. *Biofouling* **28**, 551–562 (2012).
15. Rusconi, R., Lecuyer, S., Autrusson, N., Guglielmini, L. & Stone, H. A. Secondary flow as a mechanism for the formation of biofilm streamers. *Biophys. J.* **100**, 1392–1399 (2011).
16. Rusconi, R., Lecuyer, S., Guglielmini, L. & Stone, H. A. Laminar flow around corners triggers the formation of biofilm streamers. *J. R. Soc. Interface* **7**, 1293–1299 (2010).
17. Valiei, A., Kumar, A., Mukherjee, P. P., Liu, Y. & Thundat, T. A web of streamers: biofilm formation in a porous microfluidic device. *Lab Chip* **12**, 5133–5137 (2012).
18. Weaver, W. M., Milisavljevic, V., Miller, J. F. & Di Carlo, D. Fluid flow induces biofilm formation in Staphylococcus epidermidis polysaccharide intracellular adhesin-positive clinical isolates. *Appl. Environ. Microbiol.* **78**, 5890–5896 (2012).
19. Yazdi, S. & Ardekani, A. M. Bacterial aggregation and biofilm formation in a vortical flow. *Biomicrofluidics* **6**, 044114 (2012).
20. Drescher, K., Shen, Y., Bassler, B. L. & Stone, H. A. Biofilm streamers cause catastrophic disruption of flow with consequences for environmental and medical systems. *Proc. Natl. Acad. Sci. U. S. A.* **110**, 4345–4350 (2013).
21. Hallberg, K. B., Coupland, K., Kimura, S. & Johnson, D. B. Macroscopic streamer growths in acidic, metal-rich mine waters in north wales consist of novel and remarkably simple bacterial communities. *Appl. Environ. Microbiol.* **72**, 2022–2030 (2006).
22. Hall-Stoodley, L., Costerton, J. W. & Stoodley, P. Bacterial biofilms: From the natural environment to infectious diseases. *Nat. Rev. Microbiol.* **2**, 95–108 (2004).
23. Lewandowski, Z. & Stoodley, P. Flow induced vibrations, drag force, and pressure drop in conduits covered with biofilm. *Water Sci. Technol.* **32**, 19–26 (1995).
24. Meyer-Dombard, D. R. *et al.* Hydrothermal ecotones and streamer biofilm communities in the Lower Geyser Basin, Yellowstone National Park. *Environ. Microbiol.* **13**, 2216–2231 (2011).
25. Stoodley, P., Cargo, R., Rupp, C. J., Wilson, S. & Klapper, I. Biofilm material properties as related to shear-induced deformation and detachment phenomena. *J. Ind. Microbiol. Biot.* **29**, 361–367 (2002).
26. Stoodley, P., Dodds, I., Boyle, J. D. & Lappin-Scott, H. M. Influence of hydrodynamics and nutrients on biofilm structure. *J. Appl. Microbiol.* **85**, 19s–28s (1999).
27. Stoodley, P., Lewandowski, Z., Boyle, J. D. & Lappin-Scott, H. M. Structural deformation of bacterial biofilms caused by short-term fluctuations in fluid shear: An in situ investigation of biofilm rheology. *Biotechnol. Bioeng.* **65**, 83–92 (1999).
28. Taherzadeh, D., Picioreanu, C. & Horn, H. Mass Transfer Enhancement in Moving Biofilm Structures. *Biophys. J.* **102**, 1483–1492 (2012).
29. Guillot, P., Colin, A. & Ajdari, A. Stability of a jet in confined pressure-driven biphasic flows at low Reynolds number in various geometries. *Phys. Rev. E* **78**, 016307 (2008).
30. Guillot, P., Colin, A., Utada, A. S. & Ajdari, A. Stability of a jet in confined pressure-driven biphasic flows at low Reynolds numbers. *Phys. Rev. Lett.* **99**, 104502 (2007).
31. Javadi, A., Eggers, J., Bonn, D., Habibi, M. & Ribe, N. Focus: Dripping Honey Explained. *Phys. Rev. Lett.* **110**, 144501 (2013).
32. Winstanley, H., Chapwanya, M., McGuinness, M. & Fowler, A. C. A polymer–solvent model of biofilm growth. *Proc. R. Soc. A.* **467**, 1449–1467 (2011).
33. Di Stefano, A. *et al.* Viscoelastic properties of Staphylococcus aureus and Staphylococcus epidermidis mono-microbial biofilms. *Microbiol. Biotechnol.* **2**, 634–641 (2009).
34. Hohne, D. N., Younger, J. G. & Solomon, M. J. Flexible microfluidic device for mechanical property characterization of soft viscoelastic solids such as bacterial biofilms. *Langmuir* **25**, 7743–7751 (2009).
35. Houari, A. *et al.* Rheology of biofilms formed at the surface of NF membranes in a drinking water production unit. *Biofouling* **24**, 235–240 (2008).
36. Lau, P. C., Dutcher, J. R., Beveridge, T. J. & Lam, J. S. Absolute quantitation of bacterial biofilm adhesion and viscoelasticity by microbead force spectroscopy. *Biophys. J.* **96**, 2935–2948 (2009).
37. Towler, B. W., Rupp, C. J., Cunningham, A. B. & Stoodley, P. Viscoelastic properties of a mixed culture biofilm from rheometer creep analysis. *Biofouling* **19**, 279–285 (2003).
38. Autrusson, N., Guglielmini, L., Lecuyer, S., Rusconi, R. & Stone, H. A. The shape of an elastic filament in a two-dimensional corner flow. *Phys. Fluids* **23**, 063602 (2011).
39. Roman, B. & Bico, J. Elasto-capillarity: deforming an elastic structure with a liquid droplet. *J. Phys-Condens. Mat.* **22** (2010).
40. Muppidi, S. & Mahesh, K. Study of trajectories of jets in crossflow using direct numerical simulations. *J. Fluid. Mech.* **530**, 81–100 (2005).
41. Iannitelli, A. *et al.* Potential antibacterial activity of carvacrol-loaded poly (DL-lactide-co-glycolide)(PLGA) nanoparticles against microbial biofilm. *Int. J. Mol. Sci.* **12**, 5039–5051 (2011).

Acknowledgments

AK acknowledges support from the NSERC Discovery Program. The authors would like to thank Mr. Amin Valiei for providing images used in Fig. 1(b).

Author contributions

S.D. and A.K. conceived the problem. S.D. developed the theory. S.D. and A.K. wrote the paper.

Additional information

Supplementary information accompanies this paper at http://www.nature.com/scientificreports

Competing financial interests: The authors declare no competing financial interests.

How to cite this article: Das, S. & Kumar, A. Formation and post-formation dynamics of bacterial biofilm streamers as highly viscous liquid jets. *Sci. Rep.* **4**, 7126; DOI:10.1038/srep07126 (2014).